WIRELESS COMMUNICATIONS AND MOBILE COMPUTING
Wirel. Commun. Mob. Comput. (2013)
Published online in Wiley Online Library (wileyonlinelibrary.com). DOI: 10.1002/wcm.2450

RESEARCH ARTICLE

Multi-sensor signal fusion-based modulation classification by using wireless sensor networks

Yan Zhang[1]*, Nirwan Ansari[2] and Wei Su[3]

[1] Advanced Networking Laboratory, New Jersey Institute of Technology, Newark, NJ, U.S.A.
[2] Advanced Networking Laboratory, New Jersey Institute of Technology, ECE, Newark, NJ, U.S.A.
[3] US Army Communications-Electronics RD&E Center, 6003 Combat Drive, Aberdeen Proving Grouond, MD 21005

ABSTRACT

Automatic modulation classification (AMC) is applied as the intermediate step between signal detection and demodulation to identify modulation schemes. AMC is a challenging task, especially in a non-cooperative environment, owing to the lack of prior information on the transmitted signal at the receiver. The proposed modulation classification scheme based on multi-sensor signal fusion makes the premise that the combined signal from multiple sensors provides a more accurate description than any one of the individual signals alone. Multi-sensor signal fusion offers increased reliability and huge processing gains in overall performance as compared with the single sensor, thus making AMC of weak signals in non-cooperative communication environment more reliable and successful. Signal-to-noise ratio improvement through multi-sensor signal fusion is studied by using second-order and fourth-order moments method. The classification performance based on multi-sensor signal fusion is investigated in the additive white Gaussian noise channel as well as the flat fading channel and is evaluated in terms of correct classification probability by taking the effects of timing synchronization, phase jitter, phase offset, and frequency offset into consideration, respectively. Through Monte Carlo simulations, we demonstrate that the proposed multi-sensor signal fusion-based AMC algorithm can greatly outperform other existing AMC methods.

KEYWORDS

automatic modulation classification (AMC); wireless sensor network (WSN); signal fusion

***Correspondence**

Yan Zhang, Advanced Networking Laboratory, New Jersey Institute of Technology, Newark, NJ, U.S.A.
E-mail: yz45@njit.edu

1. INTRODUCTION

Automatic modulation classification (AMC) of digital modulation formats is deployed, as the intermediate step between signal detection and demodulation, to classify the modulation schemes of the transmitted signals. Once a signal has been detected, the AMC algorithm identifies the modulation format from a pool of possible candidates. AMC has been widely studied, and many approaches have been proposed. However, AMC is still a challenging task, especially in a non-cooperative environment, owing to the lack of prior information on the transmitted signal at the receiver.

In general, typical AMC techniques can be divided into two groups: likelihood-based algorithms [1–5] and feature-based algorithms [6–15]. The likelihood-based algorithms are based on the likelihood functions (LFs) of the received signal to make modulation format decisions by testing likelihood ratios under multiple hypotheses. The typical likelihood-based algorithms include average likelihood ratio test (ALRT) [1,2], generalized likelihood ratio test [3], hybrid likelihood ratio test (HLRT) [4,5], and quasi-HLRT (QHLRT) [4]. The likelihood-based modulation decisions are optimal in the Bayesian sense, and likelihood-based classifiers have been demonstrated successfully to recognize M-ary linear digital modulation schemes, but the optimal solutions suffer from computational complexity. On the other hand, in feature-based algorithm, the decisions are made by observing the features extracted from the received signals, such as the correlation between the in-phase and quadrature signal components [6], the variance of the centered normalized signal amplitude, phase and frequency [7], the phase probability density function (PDF) [8], the variance of the zero-crossing interval [9], moments [10], cumulants [11–13], cyclic cumulants [14,15], cyclic spectrum [16], and signal

cyclostationarity [17,18]. As compared with the likelihood-based algorithms, the feature-based algorithms may not make optimal decisions, but they are usually simple to implement and can provide near-optimal performance if designed properly. A general discussion of these AMC methods based on a single sensor can be found in the survey paper [19].

Wireless sensor networks (WSNs) have been utilized for decentralized signal detection and localization [20,21] as well as estimation and classification schemes [16,22–25], primarily owing to their inherent merits, such as easy deployment and high resilience. Distributed statistical feature-based modulation classification has been discussed by using WSNs [16,22]. In the distributed cyclic spectrum feature-based AMC scheme [16], local classification decisions are made by the local radios based on the extracted cyclic spectrum features of the received signals. These local decisions are then transmitted to a fusion center, where an optimum decision rule is applied to generate the global modulation classification decision based on these local decisions and its local signal observations. The scheme proposed in [22] uses spatially distributed sensors to extract all relevant features cooperatively. The major idea behind this scheme is that individual sensors may not be able to extract all relevant features to reach a reliable classification decision; however, the cooperative in-network approach enables high classification rates at reduced overhead, even when features are noisy and/or missing. In particular, the method of multiplier [26] is employed for distributed cumulant feature extraction because of its resilience to noise and its fast convergence. Furthermore, based on the symbols collected by the WSN, a distributed clustering approach, namely method of multipliers k-means, is adopted to estimate the location of the constellation symbols. Finally, Bayesian information criterion [27] is used to determine the modulation format. One LF-based modulation classification in bandwidth constraint sensor networks has been proposed recently [23] by using WSNs. Signals are collected at each local sensor, and modulation classification decisions are made based on local received signals; the local decisions are then sent to the sensor network center to perform decision fusion to obtain the final classification result. The method proposed in [23] is currently limited to classify between two modulation schemes. Reference [24] extended this likelihood ratio test decision fusion-based modulation classification between two modulation schemes [23] to multiple modulation schemes with three different fusion algorithms, namely single selection combining, maximal-ratio combining, and equal-gain combining.

An initial study of using sensor networks for signal sensing was reported in [25]. Specially, it proposes several different types of sensor network signal sensing scenarios, including distributed sensor decision fusion, centralized synchronous signal sensing, and centralized asynchronous signal sensing. However, the classification performance of different sensing scenarios was not investigated. In this paper, we describe a novel multi-sensor signal fusion-based modulation classification scheme and perform simulations to investigate the effects of timing synchronization, phase jitter, phase offset, and frequency offset to the modulation classification performance of the signal fusion-based AMC scheme. One of the main advantages of the proposed AMC scheme is that the properly combined signal from multiple sensors provides a more accurate description than any one of the individual signals alone. Through Monte Carlo simulations, we demonstrate that the proposed multi-sensor signal fusion-based AMC scheme can surpass some other existing algorithms greatly. Other advantages of the proposed AMC scheme include the low deployment cost and basic elementary requirements on wireless sensors as compared with other modulation classification schemes by using WSNs [16,22–25]. The capacities of sensors used for modulation classification can be categorized into two types. One type of capacities is used for signal detection and transmission; this is required for all wireless sensors used for modulation classification using WSNs. The other one is used for generating modulation classification decisions, and thus, the wireless sensors are equipped with the computational, memory, and power capacity to perform this task. The capacities of wireless sensors required in the proposed signal fusion-based modulation classification scheme are simpler than other modulation classification schemes by using WSNs because the sensors used in the proposed modulation classifier only require the first basic elementary type of capacities to detect the signals, preprocess the signals simply, and transmit them to the fusion center, and do not need to generate local decisions. While in other modulation classification schemes by using WSNs [16,22–25], either some specific signal feature or local decision is made at each local sensor. Therefore, the wireless sensors deployed in the proposed signal fusion-based modulation classification scheme require less computational and memory capacity, which will reduce the deployment cost greatly. Moreover, as compared with other modulation classification schemes by using multiple sensors, the proposed AMC scheme consumes more power in signal transmission and less power in computations for feature extraction and local decision generation, because all the detected signals instead of the local decisions are transmitted to the fusion center.

The remainder of this paper is organized as follows. The multi-sensor signal fusion-based AMC scheme and the signal model are presented in Section 2. Three modulation classifiers, the cumulants-based modulation classifier, the ALRT-based modulation classifier, and the QHLRT, are described in Section 3. The numerical evaluations through Monte Carlo trials in the additive white Gaussian noise (AWGN) channel and the flat fading channel are presented in Section 4. Signal improvements through multi-sensor signal fusion are studied first. Then, modulation classification performance through multi-sensor signal fusion is investigated in terms of correct classification probability by considering the effects of timing synchronization, phase jitter, phase offset, and frequency offset. Section 5 concludes the paper.

2. MULTI-SENSOR SIGNAL FUSION-BASED MODULATION CLASSIFICATION FRAMEWORK

In this section, we describe the multi-sensor signal fusion-based modulation classification framework using a WSN. We assume a set of N_M possible modulation formats $\mathbf{M} = \{M_1, M_2, \cdots, M_{N_M}\}$. All considered modulation formats are assumed to be zero mean with unit average energy, and each of them has the same opportunity to modulate the signal to be transmitted. The goal of the modulation classifier is to determine the modulation scheme among these N_M possible modulation formats, $\mathbf{M} = \{M_1, M_2, \cdots, M_{N_M}\}$, based on the observed signal.

2.1. System model

As shown in Figure 1, a signal fusion-based AMC architecture by using a WSN can be modeled as a signal fusion center and a set of N_S distributed sensors $(J := \{J_1, J_2, \cdots, J_{N_S}\})$. A sequence of N_{sym} unknown linearly modulated signals $\{s_1, s_2, \cdots, s_{N_{sym}}\}$ is broadcast by a transmitter, where s_k denotes the k^{th} transmitted symbol, which is modulated by one unknown modulation scheme among the possible modulation format set, $\mathbf{M} = \{M_1, M_2, \cdots, M_{N_M}\}$.

The sensors are tuned to a specified frequency to collect transmitted signals. Owing to the effect of different propagations and transmission environments, N_S independent channels are assumed to connect the transmitter to these sensors, and therefore, different signals are generally observed at different receiving sensors. At each sensor $J_k (J_k \in J)$, the signals $r_k = \{r_k(1), r_k(2), \cdots, r_k(N_{sym})\}$ are collected and fed to the signal fusion center. The links between individual sensors and the signal fusion center are considered error free with sufficiently powerful error correcting codes. Thus, N_S signal vectors, $\{r_1, r_2, \cdots, r_{N_S}\}$, each of which has N_{sym} symbols, will be received, processed, and fused at the signal fusion center. The combined signal is then fed to an automatic modulation classifier for classifying the modulation format. Based on the estimated modulation scheme, the received signal is demodulated.

2.2. Signal model

After preprocessing, which involves carrier frequency and phase offset estimation and timing recovery, the received baseband signal at the sensor J_m $(m = 1, 2, \cdots, N_S)$ can be expressed as

$$r_m(n) = \sum_{k=0}^{L-1} h_m(k) s(n - k - D_m + \varepsilon_m) + g_m(n), \quad (n = 1, 2, \cdots, N_{sym}) \tag{1}$$

where $\{s(n)\}_{n=1}^{N_{sym}}$ is the transmitted symbol sequence with N_{sym} total number of the observed symbols and modulated by some unknown modulation scheme among a pool of modulation scheme $\mathbf{M} = \{M_1, M_2, \cdots, M_{N_M}\}$, $\{r_m(n)\}_{n=1}^{Nsym}$ is the received signal sequence at the sensor j_m, $\{g_m(n)\}_{n=1}^{Nsym}$ is AWGN sequence with a zero mean and a variance of σ^2, $h(k)(k = 0, 1, \cdots, L-1)$ represents the fading channel coefficient vector with length L, D_m is the transmission delay, and $\varepsilon_m \in [0, 1]$ is the timing errors parameter. Both parameters, D_m and ε_m, are different at every sensor. The AWGN channel and the flat fading channel can be modeled as a special case of fading channel with $L = 1$ as

$$r_m(n) = \begin{cases} s(n - D_m + \varepsilon_m) + g_m(n) & (AWGN\ channel) \\ \alpha_m e^{j\varphi_m} s(n - D_m + \varepsilon_m) + g_m(n) & (flat\ fading) \end{cases} \tag{2}$$

where α_m and φ_m are the channel amplitude and the phase offset in the slowly varying flat fading channel. φ_m is assumed uniformly varying within the interval $[-\pi, \pi]$. Based on the aforementioned definitions, the combined signal through multi-sensor signal fusion can be described as

$$r_F(n) = \sum_{m=1}^{N_S} b_m r_m(n) = \begin{cases} \sum_{m=1}^{N_S} b_m s(n + \Delta D_m + \Delta\varepsilon_m) + \sum_{m=1}^{N_S} b_m g_m(n) & (AWGN\ \ channel) \\ \sum_{m=1}^{N_S} b_m \alpha_m \hat{\alpha}_m^{-1} e^{j\varphi_m - j\hat{\varphi}_m} s(n + \Delta D_m + \Delta\varepsilon_m) + \sum_{m=1}^{N_S} b_m g_m(n) & (flat\ \ fading) \end{cases} \tag{3}$$

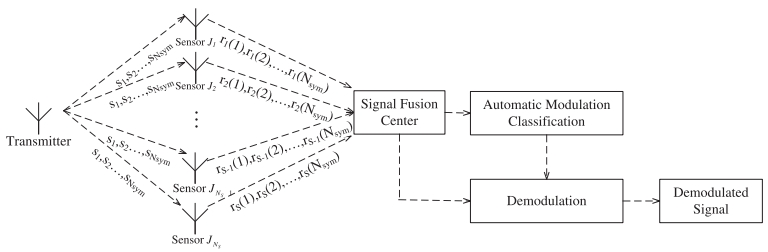

Figure 1. Multi-sensor signal fusion automatic modulation classification framework.

where $\{r_F(n)\}_{n=1}^{Nsym}$ is the combined signal sequence and b_m is the normalization factor satisfying $b_1\sigma_1 = b_2\sigma_2 = \cdots = b_{N_S}\sigma_{N_S} = \sigma$ and $b_1 + b_2 + \cdots + b_{N_S} = 1$; σ_m $(m = 1, 2, \cdots, N_S)$ is the standard deviation of the Gaussian noise received at the sensor J_m. Thus, the combined signal is a weighted sum-up of all signals collected at different sensors with more weights given to the signals with higher signal-to-noise ratios (SNRs). ΔD_m and $\Delta\varepsilon_m$ denote the transmission delay difference and time synchronization difference between the m^{th} sensor and first sensor, respectively, and $\hat{\alpha}_m$ and $\hat{\varphi}_m$ are the estimated channel amplitude and the phase offset in the slowly varying flat fading channel. In the AWGN channel, the SNR ratio of the fused signal to the signal collected at the sensor j_l can be expressed as

$$\frac{SNR_F}{SNR_l} = \frac{E\left[\left\{\left(\sum_{m=1}^{N_S} b_m s(n+\Delta D_m+\Delta\varepsilon_m)\right)^2\right\}_{n=1}^{Nsym}\right]}{E\left[\left\{\left(\sum_{m=1}^{N_S} b_m g_m(n)\right)^2\right\}_{n=1}^{Nsym}\right]} \bullet \frac{E\left[(b_l g_l(n))^2\right]}{E\left[(b_l s(n+\Delta D_m+\Delta\varepsilon_m))^2\right]} = \frac{1}{N_S b_l^2} \tag{4}$$

Assume b_M is the minimum normalization factor, $b_M = \min(b_1, b_2, \cdots, b_{N_S})$. Because $b_1 + b_2 + \cdots + b_{N_S} \geq N_S b_M$ and $b_1 + b_2 + \cdots + b_{N_S} = 1$, $b_M \leq 1/N_S$. Also, $b_1\sigma_1 = b_2\sigma_2 = \cdots = b_{N_S}\sigma_{N_S} = \sigma$, and hence, (b_M, σ_M) are the parameters corresponding to the signal with the minimum SNR. Therefore, we obtain $SNR_F \geq N_s SNR_{\min}$, implying that the SNR of the fused signal can be improved by increasing the number of the fusion sensors. In the flat fading channel, the SNR improvement of the fused signal is affected by channel estimation as shown in Equation (3).

3. TYPICAL SINGLE SENSOR-BASED MODULATION CLASSIFIERS

To demonstrate modulation classification performance improvement by using multi-sensor signal fusion, three kinds of single sensor-based modulation classifiers are simulated: the fourth-order cumulant-based classifier [11], the ALRT-based classifier [1,2], and the QHLRT-based classifier [4].

3.1. Cumulant-based classifier

The cumulant-based AMC schemes [11] have been successfully tested to classify pulse-amplitude modulation (PAM), phase-shift keying (PSK), quadrature amplitude modulation (QAM), and other modulation schemes. For a complex stationary random process $r(n)$, the p^{th} order q^{th} conjugate cumulants C_{pq} is defined as $C_{pq} = Cum\left[r^{p-q}(r^*)^q\right]$, where * denotes complex conjugation. For $p = 2$, the second-order moments are defined in two different ways:

$$\begin{aligned} C_{20} &= Cum(r(n), r(n)) = E\left[r^2(n)\right] \\ C_{21} &= Cum(r(n), r^*(n)) = E\left[|r(n)|^2\right] \end{aligned} \tag{5}$$

Similarly, for $p = 4$, the fourth-order cumulants are denoted as

$$\begin{aligned} C_{40} &= Cum[r(n), r(n), r(n), r(n)] \\ C_{42} &= Cum\left[r(n), r(n), r^*(n), r^*(n)\right] \end{aligned} \tag{6}$$

The cumulants defined in Equations (5) and (6) can be estimated from the sample estimates by replacing expectations with the sample averages over the received symbols. The sample estimates of the second-order cumulants can be written as

$$\begin{aligned} \hat{C}_{20} &= \frac{1}{N_{sym}} \sum_{k=1}^{N_{sym}} r^2(n) \\ \hat{C}_{21} &= \frac{1}{N_{sym}} \sum_{k=1}^{N_{sym}} |r(n)|^2 \end{aligned} \tag{7}$$

The normalized sample estimates of the fourth-order cumulants can also be written as

$$\begin{aligned} \hat{C}_{40} &= \left[\frac{1}{N_{sym}} \sum_{k=1}^{N_{sym}} r^4(n) - 3\left(\hat{C}_{20}\right)^2\right] / (\hat{C}_{21})^2 \\ \hat{C}_{42} &= \left[\frac{1}{N_{sym}} \sum_{k=1}^{N_{sym}} |r(n)|^4 - \left|\hat{C}_{20}\right|^2 - 2(\hat{C}_{21})^2\right] / (\hat{C}_{21})^2 \end{aligned} \tag{8}$$

3.2. Average likelihood ratio test-based classifier

The ALRT-based classifier [1,2] treats every unknown parameter as a random variable with a certain known PDF, and the LF is calculated by averaging over the unknown parameters. Assume that a series of N_{sym} received symbols $\{r_n\}_{n=1}^{Nsym}$ is received at a single sensor. The conditional PDF $p\left(r_n \left| \vec{u}, H_i \right.\right)$ of the received symbol r_n under hypothesis H_i with the unknown parameter vector $\vec{u}$ and the unknown transmitted symbol $s_n^{(i)}$ from the constellation of modulation M_i can be defined as

$$p\left(r_n \left| \vec{u}, H_i \right.\right) = (\pi N_0)^{-1} \exp\left(-N_0^{-1} \left| r_n - \alpha e^{j\varphi} s_n^{(i)} \right|^2\right) \tag{9}$$

where $\vec{u}$ is the unknown parameter vector and can be shown as $\vec{u} = (N_0, \alpha, \varphi)$. N_0, α, φ denote the noise power, the signal amplitude, and the phase offset, respectively. By averaging the conditional PDF $p\left(r_n \left| \vec{u}, H_i \right.\right)$ over constellation of the modulation M_i, the conditional LF $\Gamma\left(r_n \left| \vec{u}, H_i \right.\right)$ of the received symbol r_n under hypothesis H_i with the unknown parameter vector $\vec{u}$ can be calculated as follows

$$\Gamma\left(r_n \left| \vec{u}, H_i \right.\right) = \frac{1}{|M_i|} \sum_{k=1}^{|M_i|} (\pi N_0)^{-1} \exp \times \left(-N_0^{-1} \left| r_n - \alpha e^{j\varphi} s_k^{(i)} \right|^2 \right) \quad (10)$$

where $s_k^{(i)}$ is the k^{th} complex symbol belonging to the modulation scheme M_i that has $|M_i|$ constellation symbols, $k = 1, 2, \cdots, |M|_i$.

Then, the LF of r_n under hypothesis H_i is calculated by averaging over the unknown parameters and symbol constellation as follows:

$$\Gamma\left(r_n \left| H_i \right.\right) = \int_S \Gamma\left(r_n \left| \vec{u}, H_i \right.\right) p(\vec{u} \left| H_i \right.) d\vec{u} \quad (11)$$

where $p\left(\vec{u} \left| H_i \right.\right)$ is the *a priori* PDF of the unknown parameter vector $\vec{u}$ under the modulation scheme H_i and S is the three dimensional space for the three parameters in the unknown parameter vector $\vec{u}$.

Under the assumption of statistically independent received symbols and given a series of N_{sym} received symbols, the LF under hypothesis H_i using the ALRT-based modulation classifier can be written as the product of LFs of each received symbol $\Gamma\left(r_n \left| H_i \right.\right)$ as follows:

$$\Gamma\left(R \left| H_i \right.\right) = \prod_{n=1}^{N_{sym}} \Gamma\left(r_n \left| H_i \right.\right) \quad (12)$$

Finally, the maximum likelihood criterion, $\hat{i} = \arg\max\left(\Gamma\left(R \left| H_i \right.\right)\right), i = 1, \cdots, N_M$ where $\hat{i}$ is the index of the estimated modulation scheme of the transmitted signal, is applied to determine the modulation scheme of the received signal sequence.

3.3. Quasi-hybrid likelihood ratio test-based classifier

Using the ALRT AMC classifier, the unknown parameters are treated as random variables, and the LF is calculated by averaging over the unknown parameters and the unknown signal constellation points, while the QHLRT-based modulation classifier employs method of moments (MOMs) to estimate the unknown parameters, and the LF is computed by averaging over the unknown signal constellation points. With the QHLRT-based classifier, the LF becomes

$$\Gamma_{QHLRT}(R|H_i) = \prod_{n=1}^{N_{sym}} \frac{1}{|M_i|} \sum_{k=1}^{|M_i|} \frac{1}{\hat{N}^{(i)}} \exp \times \left\{ -\frac{1}{\hat{N}^{(i)}} \left| r_n - \hat{\alpha}^{(i)} e^{j\hat{\varphi}^{(i)}} s_k^{(i)} \right|^2 \right\} \quad (13)$$

where $\hat{\alpha}^{(i)}$, $\hat{\varphi}^{(i)}$, and $\hat{N}^{(i)}$ are the unknown parameter estimates under hypothesis H_i.

The decision rule on the modulation format of the received signal for the QHLRT-based classifier is also based on the maximum likelihood criterion, $\hat{i} = \arg\max(\Gamma_{QLRT}(R|H_i)), i = 1, \cdots, N_M$, where $\hat{i}$ is the index of the estimated modulation scheme.

4. SIMULATION RESULTS AND ANALYSES

In order to demonstrate the advantages of the proposed multi-sensor signal fusion-based AMC scheme, the classification performance of multi-sensor signal fusion-based AMC is conducted in the AWGN channel and the flat fading channel, respectively. The overall classification performance is represented in terms of the average correct classification probability. All of these classification performance analyses are based on 1000 Monte Carlo simulation trials.

4.1. Additive white Gaussian noise channel

In the AWGN channel, two modulation classification scenarios of different modulation candidate sets are considered, namely (i) {B-PSK, 4-PAM, 16-QAM, and 8-PSK} and (ii) {16-PSK and 16-QAM}. Signal improvements using multi-sensor signal fusion are studied first. By using the second-order and fourth-order moments (M_2M_4) method [28] to estimate the signal SNR, the SNR improvements of the combined quadrature PSK (Q-PSK) signal using 10-sensor signal fusion are presented. Then, the modulation classification performance based on multi-sensor signal fusion in the AWGN channel is investigated. The advantages of the proposed multi-sensor signal fusion-based modulation classifier in the AWGN channel are proved by performance comparison between the proposed multi-sensor signal fusion-based modulation classifier and single sensor cumulant-based classifier and also between the proposed AMC scheme and ALRT-based single sensor modulation classifier.

4.1.1. Signal enhancement.

To demonstrate signal enhancement through multi-sensor signal fusion, simulations are conducted by combining signals received from 100 receiving sensors with matched filters. Figure 2(a) shows the 16-QAM signal

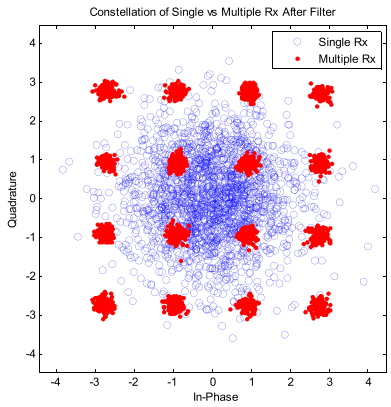

(a) 16-QAM modulation constellation comparison through single sensor versus multi-sensor with $N_S = 100$ sensors in the AWGN channel.

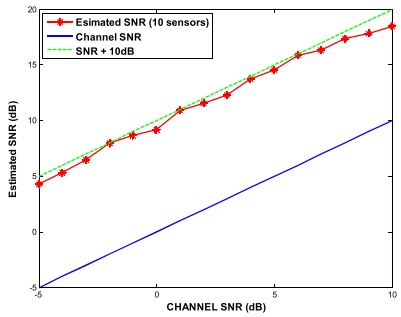

(b) QPSK signals SNR improvement with 10 sensor signal fusion in the AWGN channel.

Figure 2. Signal improvement with multi-sensor signal fusion. (a) 16-QAM modulation constellation comparison through single sensor versus multi-sensor with $N_S = 100$ sensors in the AWGN channel. (b) Q-PSK signals SNR improvement with 10-sensor signal fusion in the AWGN channel.

symbol constellation with 512 samples, which are corrupted by additive white noise with $SNR = 0$ dB and fused from multiple sensors with the matched filters at each single sensor. The blue circle dots in Figure 2(a) are the received signal symbols at a single sensor, while the red dots in this figure are the recovered symbols through multi-sensor signal fusion. From this figure, we can see that the received signal collected with a signal sensor is very noisy, while the combined signal through multi-sensor signal fusion shows a clear 16-QAM cluster constellation pattern. Constellation improvement is proved obviously by this comparison. Moreover, by using the moment-based M_2M_4 method [28], which utilizes the M_2M_4 to estimate the signal SNR, the SNR estimations of the combined Q-PSK signal through 10-sensor signal fusion are presented in Figure 2(b). From this figure, we can see that about 10 dB SNR improvement can be achieved with 10-sensor signal fusion for Q-PSK modulated signals under different channel noise conditions from −5 to 10 dB. This also conforms the theoretical analysis in Equation (4).

4.1.2. Ideal conditions.

Two experiments are implemented to verify the performance improvement of modulation classification by using WSNs in the AWGN channel under ideal conditions, implying that signals are only corrupted by the Gaussian white noise. The first experiment is based on the normalized fourth-order cumulant modulation classifier proposed in [11]. The classification performance of 10-sensor signal fusion-based fourth-order cumulant classifier is evaluated in Figure 3. The classification is carried out to distinguish among binary PSK (B-PSK), 4-PAM, 16-QAM, and 8-PSK with $N_{sym} = 100$, 250, and 500 symbols, respectively. In comparison with the classification performed by a single receiver, the average probability of correct classification is improved greatly with the multi-sensor signal fusion-based modulation classifier. More improvement can be obtained with the increase of the number of sensors, especially under low SNR conditions. As shown in Figure 3, considering the Gaussian noise only, 10-sensor signal fusion-based modulation classifier provides more than 30% improvement over the classifier with a single sensor in terms of the average correct classification probability in distinguishing the modulation formats among {B-PSK, 4-PAM, 16-QAM, and 8-PSK} under the AWGN channel in the SNR range from −5 to 0 dB. We can see from this figure that the achieved average probability of correct classification in multi-sensor signal fusion-based modulation classifier with 10 sensors at −5 dB SNR point is almost the same as that of the single sensor-based classifier at 3 dB SNR point.

The performance of the multi-sensor signal fusion-based ALRT modulation classifier [1,2] is evaluated in the framework comprising different numbers of sensors. The detectors implemented for local sensors are identical. The classification is carried out to distinguish between 16-PSK and square-shaped 16-QAM signals in situations

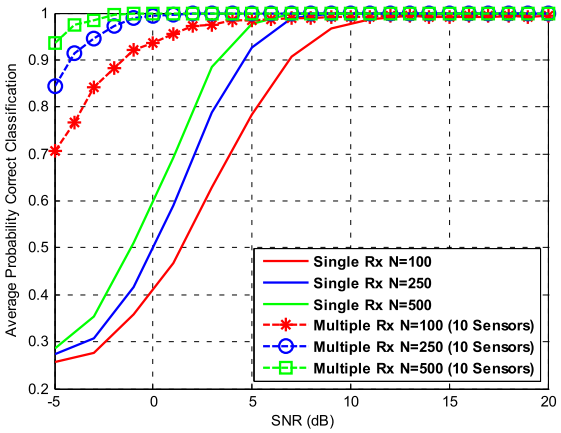

Figure 3. B-PSK, 4-PAM, 16-QAM, and 8-PSK modulation classification performance comparison of cumulant-based classifier and multi-sensor signal fusion-based classifier with $N_S = 10$ sensors and $N_{sym} = 100$, 250, and 500, respectively, in the AWGN channel.

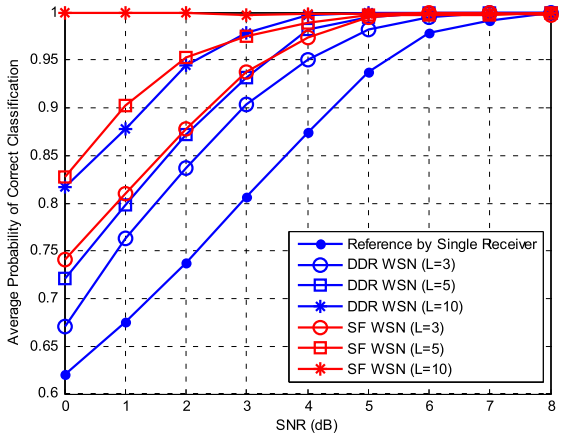

Figure 4. 16-PSK and 16-QAM modulation classification performance comparison of distributed decision ratio-based AMC classifier and multi-sensor signal fusion-based classifier with $N_S = 3$, 5, and 10 sensors and $N_{sym} = 100$ in the AWGN channel.

where the carrier phase offset is unknown to all of the sensors. Each emitted symbol is corrupted by additive white noise. The theoretical counterpart derived for the single receiver is plotted here for comparison purposes. In comparison with the classification performance achieved by a single sensor, the average probabilities of correct classification with multi-sensor signal fusion-based modulation classifier, which is presented with the curves named "SF WSN" in Figure 4, exhibit great improvements. At 0 dB, more than 10%, 20%, and 30% improvement of the average probabilities of correct classification can be achieved with signal fusion-based modulation classifier with 3 sensors, 5 sensors, and 10 sensors than the single sensor-based ALRT classifier, respectively. The achieved average probabilities of correct classification in signal fusion-based modulation classifier with 3 sensors, 5 sensors, and 10 sensors at 0 dB are almost the same as those with the single sensor-based ALRT classifier at 2, 3, and 8 dB, respectively. We also compare the performance of the proposed multi-sensor signal fusion-based modulation classification scheme with the distributed decision ratio-based modulation classifier using WSNs proposed in Reference [23], the simulation results of which are denoted as "DDR WSN" in Figure 4. As compared with the classification performance with distributed decision ratio-based classifier, about 5% and 10% correct classification probability improvements can be achieved at low SNR with three sensors and five sensors signal fusion-based modulation classifier, respectively.

The performance improvement in the low SNR range in these two simulations under the ideal AWGN channel conditions is due to the SNR improvement of the combined signal. As shown in Equation (4), the SNR of the fused signal under ideal condition can be improved by increasing the number of the sensors, as validated in Figures 3 and 4. Moreover, as shown in Figure 2(b), the estimated SNR by using the 512 samples of the combined signal sequences collected with 10 sensors can be improved by around 8 dB under the ideal condition. The modulation classifier with a single sensor can almost correctly distinguish the modulation formats among {B-PSK, 4-PAM, 16-QAM, and 8-PSK} and {16-PSK and 16-QAM} under 3 and 8 dB SNR channel conditions, as indicated in the green curve and the blue solid dot curve in Figures 3 and 4, respectively. Hence, the signal fusion-based modulation classifier with 10 sensors can almost identify the modulation formats at −5 and 0 dB in these two evaluations, shown in the green square curve and the red star curve in Figures 3 and 4, respectively.

4.1.3. Timing synchronization.

Because all the signal sequences collected at different sensors need to be transmitted to the signal fusion center to perform signal fusion and modulation classification, the proposed multi-sensor signal fusion-based modulation classifier is a centralized modulation classification scheme. As shown in Equation (3), the combined signal through multi-sensor signal fusion is a weighted sum-up of the signal sequences collected at different sensors. Hence, the proposed multi-sensor signal fusion-based modulation classification scheme suffers from two types of timing synchronization. One is the timing synchronization between the unknown transmitter and each local sensor, and the other one is the synchronization between different sensors. On the contrary, the distributed modulation classification schemes with multiple sensors only suffer from the former type of timing synchronization because the local decisions, which are made based on the collected signal sequence at each local sensor, are transmitted to the fusion center. Thus, the distributed modulation classification schemes with multiple sensors do not suffer from the timing synchronization between different sensors. In this part, we study the effects of timing synchronization on the performance of the proposed modulation classification scheme. With $S = 10$ sensors and $SNR = 10$ dB, B-PSK, 4-PAM, 16-QAM, and 8-PSK multi-sensor signal fusion cumulant-based modulation classification performance P_c against timing errors ε_T is plotted in Figure 5, with $N_{sym} = 100$, 250, and 500 symbols, respectively, in the AWGN channel. With square timing-based blind delay recovery [29] at each local sensor and synchronization between sensors, classification performance can be maintained with timing errors $[-0.2T, 0.2T]$. Notice that over 94% correct classification probability can still be obtained even with $0.2T$ timing errors.

4.1.4. Phase jitter.

To study the robustness of multi-sensor signal fusion-based modulation classification scheme to phase jitter, classification performance P_c among {B-PSK, 4-PAM, 16-QAM, and 8-PSK} is plotted against Φ in Figure 6, with $N = 200$ samples and $SNR = 12$ dB for single and 10 sensors in the AWGN channel. The phase $\varphi_l^{(m)}$ is assumed to be uniformly distributed over $[-\Phi, \Phi]$ and

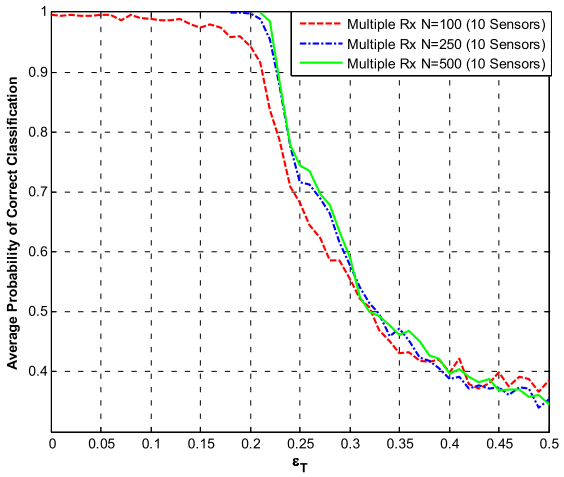

Figure 5. B-PSK, 4-PAM, 16-QAM, and 8-PSK modulation classification performance comparison of cumulant-based classifier and multi-sensor signal fusion-based classifier with $N_S = 10$ sensors and $N_{sym} = 100$, 250, and 500, respectively, in the AWGN channel.

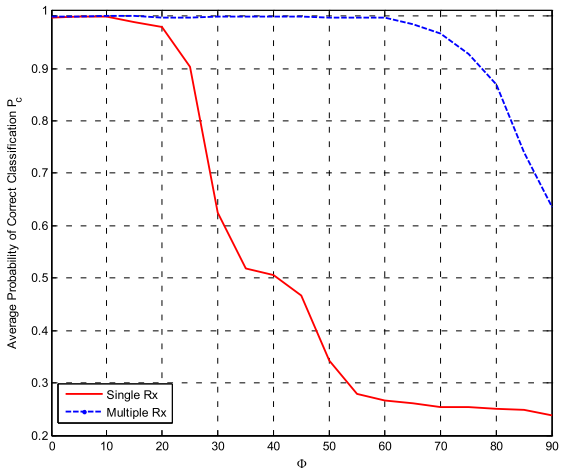

Figure 6. Average correct classification probability P_c versus Φ for {B-PSK, 4-PAM, 16-QAM, and 8-PSK}, the l^{th} symbol's phase jitter at m^{th} sensor $\theta_l^{(m)}$ is uniformly distributed over [-Φ,Φ] and $N_{sym} = 200$, $SNR = 12$ dB in the AWGN channel.

varies from sensor to sensor and from symbol to symbol. Performance degradation caused by phase jitter of single sensor cumulant-based modulation classifier has been studied in Reference [11]. For comparison, the results are also shown as the red curve in Figure 6. For a single sensor, acceptable performance is obtained for $\Phi < 30°$; as Φ is greater than 30°, P_c drops very sharply. With 10-sensor signal fusion-based modulation classifier, the performance is still acceptable even with large Φ.

4.1.5. Phase offset.

How performance is affected by phase offset of single sensor cumulant-based modulation classifier has been

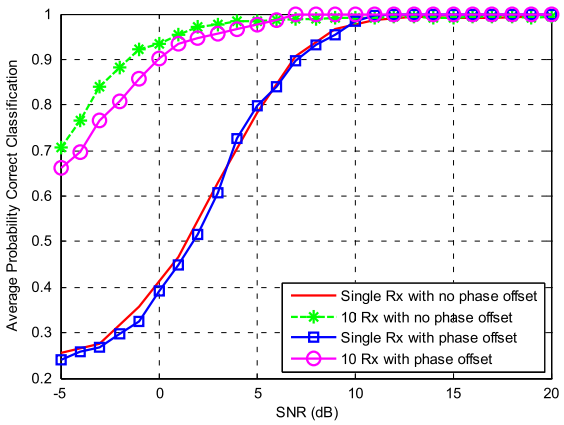

Figure 7. Average correct classification probability P_c versus SNR for {B-PSK, 4-PAM, 16-QAM, and 8-PSK}, phase offset at m^{th} sensor φ_m varies randomly over $[-\pi, \pi]$ from realization to realization, and $N_{sym} = 200$ in the AWGN channel.

studied in Reference [11]. According to their investigations, there is no obvious degradation in classification performance with the effects of phase offset by using single receiver cumulant-based classifier. Phase offset varies randomly over the range $[-\pi, \pi]$ in one realization. The average correct classification probability P_c is plotted against SNR in Figure 7, with $N = 200$ samples for single and 10 sensors in the AWGN channel among B-PSK, 4-PAM, 16-QAM, and 8-PSK modulation schemes. The existence of phase offset causes the signal constellation to rotate by an angle of phase offset, and therefore, before the signal fusion, phase offset needs to be removed. The M-Power method [30] is used for carrier phase recovery, which is a non-data-aided method. In the multiple-receiver scheme, phase offset φ_m is different at each local receiver but fixed at one local receiver over a realization. Note that in Figure 7, there is almost no degradation in classification performance with high SNR. With low SNR, classification performance is degraded by about 5% because of phase recovery error. Performance improvement of multi-sensor signal fusion-based modulation classification scheme is degraded by phase offset recovery at low SNR; however, the whole classification performance is still improved as compared with the single sensor classifier.

4.1.6. Frequency offset.

Frequency offset influences on the classification performance are further studied. Like phase offset, frequency offset also causes the rotation of the signal constellations; thus, frequency offset needs to be removed before the signal fusion. Performance degradation of single sensor cumulant-based modulation classifier by frequency offset has been studied in Reference [11]. The average correct classification probability P_c is plotted against the normalized frequency offset f_0 in Figure 8. The same simulation condition is assumed as in [11]: The number of symbols is $N = 250$, $SNR = 12$ dB, and the normalized

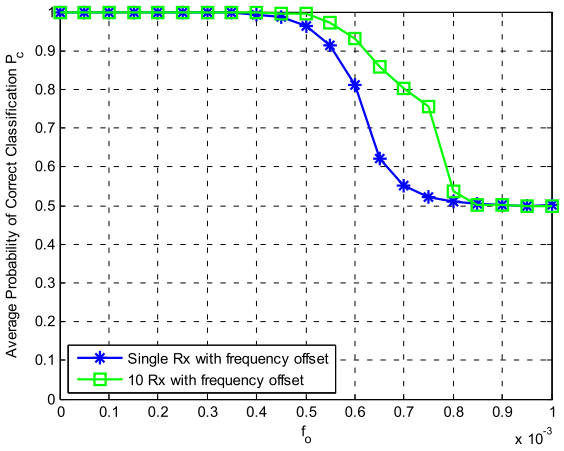

Figure 8. Average probability of correct classification P_c versus frequency offset f_0 for {B-PSK, 4-PAM, 16-QAM, and 8-PSK} modulation classification with $N_{sym} = 250$ symbols and $SNR =$ 12 dB in the AWGN channel without frequency offset.

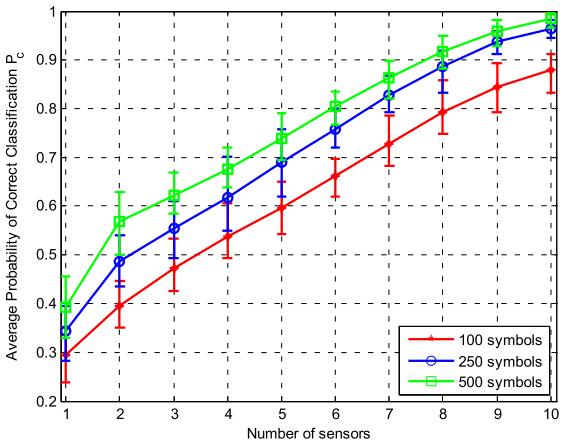

Figure 9. Average probability of correct classification P_c versus number of sensors for {B-PSK,} {4−*PAM*, 16−*QAM*, } { *and* 8 − *PSK*} modulation classification with $SNR = [-5$ dB, 0 dB] and $N_{sym} = 100, 250,$ and 500 symbols, respectively, in the AWGN channel.

frequency offset f_0 varies from 0 to 0.001 (corresponding to a maximum rotation of 90°). According to their results, acceptable performance for single sensor cumulant-based modulation classifier is obtained for $f_0 < 0.6 \times 10^{-3}$. As compared with single sensor, there is more than 10% classification performance improvement with the normalized frequency offset f_0 in the range of $[0.6, 0.75] \times 10^{-3}$, but under high frequency offset condition, there is no improvement on the classification performance even with more sensors signal fusion; so, some kind of frequency offset recovery technique is required to improve the classification performance further.

4.1.7. Noise variance.

In practice, sensors at different locations will experience different noise levels, implying that the SNR value at different sensors should be different. In order to investigate the effects of noise variance to signal fusion-based AMC scheme, a further experiment is performed in the AWGN channel to classify among {B-PSK, 4-PAM, 16-QAM, and 8-PSK} modulation schemes with 100, 250, and 500 symbols, SNR varying in the range of [−5 dB, 0 dB], and the number of sensors varying from 1 to 10. Signals with very low SNR (smaller than −5 dB) can be singly discarded from signal fusion. The average correct classification probability P_c is plotted against the number of sensors in Figure 9. No timing issue, phase jitter, phase offset, and frequency offset are considered here. The results in Figure 9 show that the correct classification probability is within some range of the average value ($< \pm 0.05$), and therefore, multi-sensor signal fusion-based AMC scheme is tolerant to noise variance at different sensor locations.

4.2. Flat fading channel

In the flat fading channel, the performance of the proposed scheme is compared with the QHLRT-based modulation classifier with the MOM estimator and the ALRT-based classifier with the perfect unknown parameters estimator. In Figure 10, the classification performance for the ALRT-based classifier under the assumption of perfect estimations of unknown channel amplitude and phase offset parameters, the QHLRT-based classifier with the MOM estimator, and the proposed multi-sensor signal fusion-based classifier with MOM estimations of unknown parameters in the flat Rayleigh fading is presented, with 100 and 1000 symbols, respectively. The classification is carried out to distinguish among B-PSK, Q-PSK, 8-PSK, and

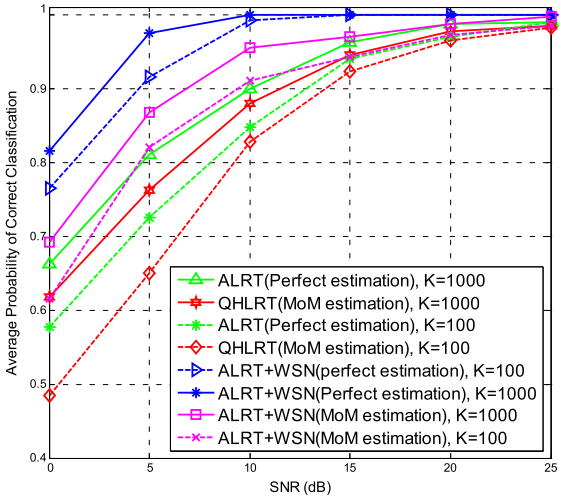

Figure 10. B-PSK, Q-PSK, 8-PSK, and 16-PSK modulation classification performance comparison of QLRT-based classifier and multi-sensor signal fusion-based classifier in the flat Rayleigh fading channel with $N_S = 10$ sensors, $N_{sym} = 100$ and 1000 symbols, respectively.

16-PSK modulation formats in the situations where the carrier phase offset is unknown to all of the sensors. Each emitted symbol is rotated by a randomly generated carrier phase, which is a constant value across N_{sym} symbols over the flat Rayleigh fading channel and corrupted by white noise. Therefore, signal constellation rotations have to be removed before signal fusion. For comparison, classification performances with a single receiving sensor by the ALRT-based classifier with perfect estimation of unknown parameters and the QHLRT-based classifier with MOM unknown parameter estimates are also presented. From Figure 10, we can see that with perfect unknown parameter estimates, more than 15% of the average probability of correct classification can be achieved at 0 dB with 10-sensor signal fusion-based classifier than a single sensor-based ALRT classifier, while by using MOM-based unknown parameter estimates, more than 10% of the average probability of correct classification can be achieved at 0 dB with 10-sensor signal fusion-based classifier than a single sensor-based QHLRT classifier. It can also be noticed that the average probabilities of correct classification with MOM estimates are smaller than that with perfect unknown parameter estimates due to the unknown parameter estimation errors.

5. CONCLUSION AND FUTURE WORK

In this paper, we have proposed and studied WSNs-based multi-sensor signal fusion to automatically detect modulation schemes in the AWGN channel and the flat fading channel. The AMC of weak signals in non-cooperative communication environment becomes more reliable and successful by using multi-sensor signal fusion. The classification performance of the proposed scheme is evaluated in terms of correct classification probability. Through Monte Carlo simulations, we demonstrate that the proposed multi-sensor signal fusion-based AMC scheme can surpass other existing algorithms greatly in the AWGN channel and the flat fading channel. However, the classification performance of the proposed modulation classification scheme based on multi-sensor signal fusion in multipath fading channel needs further investigations. Also, because all the signal sequences need to be transmitted to the signal fusion center to perform signal fusion and modulation classification, wireless bandwidth constraint is an issue to be considered in the signal fusion-based modulation classification scheme. As compared with the signal fusion-based AMC scheme, decision fusion-based modulation classification schemes can alleviate the bandwidth burden because only the local decisions, which consume much less bandwidth than the received signal sequences, will be transmitted to the fusion center. However, the deployment cost of decision fusion-based AMC scheme is much higher than that of signal fusion-based AMC method because more capable wireless sensors are required to make local decisions in the decision fusion-based AMC scheme, while the operations of wireless sensors in the signal fusion-based modulation classification scheme are quite simple and no decision fusion is made at the local sensor. Moreover, the distributed fusion-based AMC scheme, which takes advantages of both signal fusion and decision fusion, is also worth further investigation.

REFERENCES

1. Sills JA. Maximum-likelihood modulation classification for PSK/QAM, In *Proceedings of Military Communications Conference (MILCOM)*, vol. 1, Atlantic City, NJ, Oct. 1999; 217-220.
2. Wei W, Mendel JM. Maximum-likelihood classification for digital amplitude-phase modulations. *IEEE Transactions on Communications* 2000; **48**: 189–193.
3. Panagiotou P, Anastasopoulos A, Polydoros A. Likelihood ratio tests for modulation classification, In *Proceedings of IEEE Military Communications Conference Proceeding (MILCOM)*, vol. 2, Los Angeles, California, USA, October 22-25, 2000; 670–674.
4. Dobre OA, Hameed F. Likelihood-based algorithms for linear digital modulation classification in fading channels, In *Proceedings of IEEE Canadian Conference on Electrical and Computer Engineering (CCECE), 2006*, Ottawa, Canada, May 7–10, 2006; 1347–1350.
5. Hameed F, Dobre O, Popescu D. On the likelihood-based approach to modulation classification. *IEEE Transactions on Wireless Communications* Dec. 2009; **8**(12): 5884–5892.
6. Dobre OA, Abdi A, Bar-Ness Y, Su W. The classification of joint analog and digital modulations, In *Proceedings of Military Communications Conference (MILCOM)*, Atlantic City, NJ, USA, 2005; 1–6.
7. Azzouz EE, Nandi AK. *Automatic Modulation Recognition of Communication Signals*. Kluwer Academic: Norwell, MA, USA, 1996.
8. Yang Y, Liu C-H. An asymptotic optimal algorithm for modulation classification. *IEEE Communications Letters* May 1998; **2**(5): 117–119.
9. Hsue SZ, Soliman SS. Automatic modulation classification using zero crossing. *IEEE Radar and Signal Processing* 1990; **137**: 459–464.
10. Dai W, Wang Y, Wang J. Joint power estimation and modulation classification using second- and higher statistics, In *Proceedings of IEEE Wireless Communications and Networking Conference (WCNC)*, Orlando, FL, USA, March 17–21, 2002; 155-158.
11. Swami A, Sadler BM. Hierarchical digital modulation classification using cumulants. *IEEE Transactions Communications* 2000; **48**: 416–429.
12. Spooner CM. On the utility of sixth-order cyclic cumulants for RF signal classification, In *the thirty-fifth*

Asilomar Conference on Signals, Systems and Computers, 2001, Asilomar Conference Centre Asilomar Pacific Grove, California, USA, July 8–13, 2001; 890-897.
13. Wu H-C, Saquib M, Yun Z. Novel automatic modulation classification using cumulant features for communications via multipath channels. *IEEE Transactions on Wireless Communications* 2008; **7**(8): 3098–3105.
14. Dobre OA, Bar-Ness Y, Su W. Robust QAM modulation classification algorithm based on cyclic cumulants, In *Proceedings of IEEE Wireless Communications and Networking Conference (WCNC)*, Atlanta, Georgia, USA, March 21–25, 2004; 745-748.
15. Dobre OA, Oner M, Rajan S, Inkol R. Cyclostationarity-based robust algorithms for QAM signal identification. *IEEE Communications Letters* January 2012; **16**(1): 12–15.
16. Headley WC, Reed JD, da Silva CRC. Distributed cyclic spectrum feature-based modulation classification, In *Proceedings of IEEE Wireless Communications and Networking Conference(WCNC)*, Las Vegas, NV, March 31- April 3, 2008; 1200-1204.
17. Punchihewa A, Zhang Q, Dobre OA, Spooner C, Rajan S, Inkol R. On the cyclostationarity of OFDM and single carrier linearly digitally modulated signals in time dispersive channels: theoretical developments and application. *IEEE Transactions on Wireless Communications* August 2010; **9**(8): 2588–2599.
18. Al-Habashna A, Dobre OA, Venkatesan R, Popescu DC. Second-order cyclostationarity of mobile WiMAX and LTE OFDM signals and application to spectrum awareness in cognitive radio systems. *IEEE Journal of Selected Topics in Signal Processing* February 2012; **6**(1): 26–42.
19. Dobre OA, Abdi A, Bar-Ness Y, Su W. Survey of sutomatic modulation classification techniques: classical approaches and new trends. *IET Communications* April 2007; **1**: 137–156.
20. Chen H, Wang G, Wang Z, So HC, Poor HV. Non-line-of-sight node localization based on semi-definite programming in wireless sensor networks. *IEEE Transactions on Wireless Communications* January 2012; **11**(1): 108–116.
21. Wang G, Chen H. An importance sampling method for TDOA-based source localization. *IEEE Transactions on Wireless Communications* May 2011; **10**(5): 1560–1568.
22. Forero PA, Cano A, Giannakis GB. Distributed feature-based modulation classification using wireless sensor networks, In *Proceedings of IEEE Military Communications Conference (MILCOM)*, San Diego, CA, November 2008; 1–7.
23. Xu JL, Su W, Zhou M. Distributed automatic modulation classification with multiple sensors. *IEEE Sensor Journal* 2010; **10**(11): 1779–1785.
24. Xu JL, Su W, Zhou M. Asynchronous and high-accuracy digital modulated signal detection by sensor networks, In *Proceedings of IEEE Military Communications Conference (MILCOM)*, Baltimore, MD, USA, November 7–10, 2011; 589–594.
25. Su W, Kosinski J. Framework of network centric signal sensing for automatic modulation classification, In *Proceedings of IEEE International Conference on Networking, Sensing, and Control*, Chicago, Illinois, USA, April 11–13, 2010; 534–539.
26. Bertsekas DP, Tsitsiklis JN. *Parallel and Distributed Computation: Numerical Methods*. Athena Scientific: Belmont, Massachusetts, 1997.
27. Kass RE, Wasserman L. A reference Bayesian test for nested hypotheses and its relationship to the Schwarz criterion. *Journal of the American Statistical Association* 1995; **90**(431): 928–934.
28. Pauluzzi DR, Beaulieu NC. A comparison of SNR estimation techniques for the AWGN channel. *IEEE Transactions on Communications* 2000; **48**: 1681–1691.
29. Oerder M, Myer H. Digital filter and square timing recovery. *IEEE Transactions on Communications* May 1988; **COM-36**(5): 605–612.
30. Mengali U, D'Andrea AN. *Synchronization Techniques for Digital Receivers*. Plenum Press: New York, 1997.

AUTHORS' BIOGRAPHIES

Yan Zhang received the BE and ME degrees in Electrical Engineering from Shandong University, China, in 2001 and 2004, respectively. She is currently pursuing her PhD degree in Computer Engineering in the Department of Electrical and Computer Engineering at New Jersey Institute of Technology, Newark, New Jersey. Her research interests include congestion control and energy optimization in data center networks, content delivery acceleration over wide area networks, and energy efficient networking.

Nirwan Ansari received BSEE (summa cum laude with a perfect GPA) from New Jersey Institute of Technology (NJIT), MSEE from University of Michigan, Ann Arbor, and PhD from Purdue University, West Lafayette, IN. He joined NJIT's Department of Electrical and Computer Engineering as an

assistant professor in 1988 and has been a full professor since 1997. He has also assumed various administrative positions at NJIT. He has been a visiting (chair) professor at several universities. Prof. Ansari authored Media Access Control and Resource Allocation (Springer, 2013) with J. Zhang and Computational Intelligence for Optimization (Springer, 1997) with E. S. H. Hou and edited Neural Networks in Telecommunications (Springer, 1994) with B. Yuhas. He has also contributed over 450 technical papers, over one third of which were published in widely cited refereed journals/magazines. He has guest edited a number of special issues, covering various emerging topics in communications and networking. His current research focuses on various aspects of broadband networks and multimedia communications. Prof. Ansari has served on the Editorial Board and Advisory Board of nine journals. He was elected to serve in the IEEE Communications Society (ComSoc) Board of Governors as a member at large (2013–2015). He has chaired ComSoc technical committees and has been actively organizing numerous IEEE International Conferences/Symposia/Workshops, assuming various leadership roles. Some of his recognitions include IEEE Fellow (Class of 2009), several Excellence in Teaching Awards, a couple of best paper awards, Thomas Alva Edison Patent Award (2010), NJ Inventors Hall of Fame Inventor of the Year Award (2012), 2013 Outstanding Service Recognition Award (ComSoc AHSN TC), and designation as an IEEE Communications Society distinguished lecturer (2006–2009, two terms). He has also been granted over 20 US patents.

Wei Su received the BS degree in Electrical Engineering and the MS degree in Systems Engineering from Shanghai Jiao Tong University, China, in 1983 and 1987, respectively. He received his ME and PhD degrees in electrical engineering from The City University of New York, USA, in 1992. Since 1991, he has worked with US Army Research Laboratory and US Army Communication-Electronics Research Development and Engineering Center (CERDEC). His research interest includes blind signal exploitation, wireless sensor network, cognitive radios, signal and image processing, modeling and simulation, adaptive control and automation, and frequency control and timing devices. Dr. Su is a recipient of many awards including US Army Superior Civilian Service Award and Medal, Association of Old Crows Research and Development Award, IEEE Region I Award for contributions to military communications and electronic warfare technology, US Army Research and Development Achievement Award, US Army Material Command Top 10 Employee Nomination, Thomas Alva Edison Patent Award, US Army Performance Achievement Awards, Electronic Warfare and Information Operation Technology Hall of Fame, US Army CERDEC Inventor's Wall of Honor, and US Army CERDEC Innovator's Gold Award. He is a fellow of the IEEE Communications Society.